Ultrafast magnetization dynamics rates within the Landau-Lifshitz-Bloch model

U. Atxitia and O. Chubykalo-Fesenko

Instituto de Ciencia de Materiales de Madrid, CSIC, Cantoblanco, ES-28049 Madrid, Spain

(Received 19 November 2010; revised manuscript received 18 February 2011; published 10 October 2011)

Ultrafast laser-induced magnetization dynamics is analyzed in terms of the Landau-Lifshitz-Bloch (LLB) equation for different values of spin S. Within the LLB model the ultrafast demagnetization time (τ_M) and the transverse damping ($\alpha_\perp$) are parametrized by the intrinsic coupling-to-the-bath parameter λ, defined by the microscopic spin-flip rate. We show that the LLB model is equivalent to a recently introduced M3TM model [B. Koopmans *et al*., Nature Mat. **9**, 259 (2010)] with $S = 1/2$ within the assumption that the intrinsic scattering mechanism is the phonon-mediated Elliott-Yafet scattering. As a result, for this process λ is proportional to the ratio between the nonequilibrium phonon and electron temperatures, in contrast to previous models with $\lambda = \text{const}$. We investigate the influence of the finite spin number and the scattering rate parameter λ on the ultrafast magnetization dynamics. The differences in the demagnetization time scale in transition metals and Gd are attributed to the fact that this parameter is almost two orders of magnitude smaller in the latter case. The relation between the femtosecond demagnetization rate and the perpendicular picosecond–nanosecond damping, provided by the LLB theory, is checked based on the available experimental data. A good agreement is obtained for Ni, Co, and Gd, providing validation of the LLB model.

DOI: 10.1103/PhysRevB.84.144414 PACS number(s): 75.40.Gb, 75.70.−i

I. INTRODUCTION

Magnetization precession and spin-phonon relaxation rates on picoseconds time scale were considered to be the limiting factors for the speed of the magnetization switching,[1,2] until it was demonstrated that optical excitation with fs pulsed lasers could influence the magnetization on femtosecond timescale.[3–6] Ultrafast laser-induced demagnetization immediately became a hot topic in solid state physics due to an appealing possibility to further push the limits of operation of magnetic devices.[7] This ultrafast process has now been shown to proceed with several important characteristic time scales:[6] (i) a femtosecond demagnetization with time scale τ_M, (ii) a picosecond recovery with time scale τ_E, and (iii) a hundred-picosecond to nanosecond magnetization precession and relaxation, traditionally characterized by the ferromagnetic resonance frequency ω_{FMR} and the Landau-Lifshitz-Gilbert damping parameter α_{LLG} ($\alpha_\perp$) (see Fig. 1).

The correct account for the physics of the magnetization changes on femtosecond time scales is obviously not trivial and requires the time-dependent relativistic quantum mechanics within a many-body approach. An important problem is the open question of the role of different subsystems (photons, phonons, electrons, and spins) in the ultrafast angular momentum transfer.[8] This common goal is stimulated by experimental findings provided by X-ray Magnetic Circular Dichroism (XMCD) measurements showing the important role of spin-orbit interactions.[9,10] While some degree of understanding has been achieved in *ab initio* modeling of the ultrafast demagnetization (τ_M) scale,[9,11–15] modeling all three ultrafast magnetization dynamics rates within the same approach is outside the possibilities of quantum mechanical approaches.

The three-temperature (3T) phenomenological model involves the rate equations for the electron, phonon, and spin temperatures (energies).[11,16–18] It has been shown that the introduction of the spin temperature is not adequate[19] since the spin system is not in equilibrium on the femtosecond time scale. It has been suggested to couple the spin dynamics to the two-temperature (2T) model for phonon and electron temperatures.[19–23] These models are based on the energy flow picture and leave unidentified the angular momentum transfer mechanism and the underlying quantum mechanism responsible for the spin flip.[23] They essentially interpret the ultrafast demagnetization as "thermal" processes, understanding the temperature as energy input from photon to electron and then to the spin system. By using these models the important role of the linear reversal path in the femtosecond demagnetization has been identified.[24,25] The comparison with experiment seems to indicate that in order to have magnetization switching on the ultrafast time scale, a combined action of "heat" and large field coming from the inverse Faraday effect is necessary.[25]

The most successful recent phenomenological models describing ultrafast magnetization dynamics are (i) Langevin dynamics based on the Landau-Lifshitz-Gilbert (LLG) equation and the classical Heisenberg Hamiltonian for localized atomic spin moments,[19,20] (ii) Landau-Lifshitz-Bloch (LLB) micromagnetics,[22,23] and (iii) Koopmans' magnetization dynamics model (M3TM).[26] The spin dynamics could be coupled to the electron temperature from the 2T model, underlying the electronic origin of the spin-flip process[19,20,22,23,25] or to both electron and phonon temperatures, underlying the Elliott-Yafet mechanism mediated by phonons.[26] When the 2T model was carefully parametrized from the measured reflectivity, this approach gave excellent agreement with the experiment in Ni (Ref. 23) using the former mechanism or in Ni, Co, and Gd using the latter mechanism.[26]

In the classical derivation of the LLB equation thermal averaging is performed analytically within the mean-field approximation (MFA).[27] Thus, the LLB equation for classical spins ($S \to \infty$) is equivalent to an ensemble of exchange-coupled atomistic spins modeled by stochastic LLG equations.[21,28] At the same time, in some cases the LLB equation may be preferable with respect to the atomistic Heisenberg model, since being micromagnetic it can incorporate the quantum

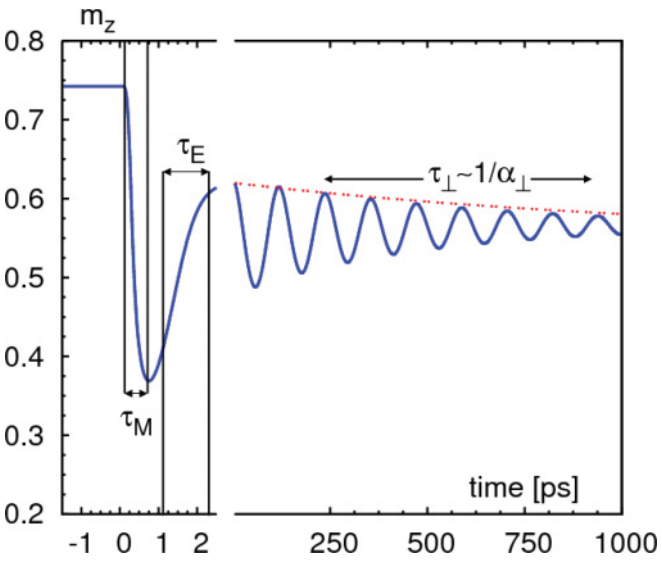

FIG. 1. (Color online) Characteristic time scales in ultrafast laser-induced magnetization dynamics experiments. The curve is obtained by the integration of the Landau-Lifshitz-Bloch equation coupled to the two-temperature model with the parameters from Ref. 22. For the modeling of precession the applied field $H_{ap} = 1$ T at 30 degrees was used.

nature of magnetism and the quantum derivation of LLB also exists.[29] In particular, the limits of validity for the statistical mechanics based on the classical Heisenberg model for the description of materials with delocalized magnetism of d electrons in transition metals or magnetism of f electrons in rare earths are not clear. An alternative statistical simplified description of d metals consists of a two-level system with spin-up and spin-down bands (i.e., $S = \pm 1/2$), as has been proposed by Koopmans *et al.*[26] Their model, as we show in the present paper, is also equivalent to the quantum LLB equation with spin $S = 1/2$. An additional advantage of using the LLB equation is the possibility of modeling larger spatial scales.[21,22] Therefore LLB micromagnetics is an important paradigm within the multiscale magnetization dynamics description. The LLB equation has been shown to describe correctly the three stages of ultrafast demagnetization processes: the subpicosecond demagnetization, the picosecond magnetization recovery, and the nanosecond magnetization precession[21–23] (see Fig. 1).

The intrinsic quantum mechanical mechanisms responsible for ultrafast demagnetization in the LLB model are included in the intrinsic coupling-to-the-bath parameter λ.[23,29] The coupling process is defined by the rate of spin flip. Several possible underlying quantum mechanisms are currently under debate: the Elliott-Yafet (EY) electron scattering mediated by phonons or impurities[14,26] or other electrons[15] and electron-electron inelastic exchange scattering.[30,31] By combining the macroscopic demagnetization equation (M3TM model) with the rate of spin flip calculated on the basis of the full Hamiltonian, Koopmans *et al.*[26] have been able to relate the ultrafast demagnetization time τ_M with the spin flip rate of the phonon-mediated Elliott-Yafet scattering. The authors fitted experimental demagnetization rates in Ni, Co, and Gd to the phenomenological M3TM model and found them to be consistent with the values estimated on the basis of *ab initio* theory.[14] The coupling-to-the-bath parameter λ (microscopic damping parameter in the atomistic LLG model) should be distinguished from that of the macroscopic damping α_{LLG} ($\alpha_\perp$ in the LLB model), a more complicated quantity which includes the magnon-magnon processes.

The first attempt to relate the subpicosecond demagnetization time to the macroscopic damping processes was given by Koopmans *et al.*,[6] who suggested the relation $\tau_M \sim 1/\alpha_{LLG}$. Subsequently and with the aim of checking this relation, several experiments in doped permalloy were performed.[32–34] The permalloy thin films were doped with rare-earth impurities, allowing the damping parameter α_{LLG} to be increased in a controlled way. The effect on the demagnetization time τ_M was shown to be opposite[34] or null,[32] in contrast to the above relation. However, it should be noted that the analysis leading to this expression was performed in terms of the Landau-Lifshitz-Gilbert equation, relating the ultrafast demagnetization time τ_M to the transverse damping without taking into account their temperature dependence. Moreover, one should take into account that the rare-earth impurities may introduce a different spin-flip mechanism with a slower time scale.[33]

Partially based on the above-mentioned experimental results and from a general point of view, the longitudinal relaxation (the ultrafast demagnetization rate τ_M) and the transverse relaxation (the LLG damping α_{LLG}) may be thought to be independent quantities. Indeed, different intrinsic and extrinsic mechanisms can contribute to the magnetization dynamics rates at different time scales. One can, for example, mention that during the femtosecond demagnetization the electron temperature is often raised to the Curie temperature.[23,25] At this moment, high-frequency terahertz spin waves[35,36] including Stoner excitations[31] contribute. At the same time, the transverse relaxation is related to the homogeneous precessional mode at lower temperatures. The LLB equation takes care of the different natures of longitudinal and transverse relaxation, arising from the spin disordering. The LLB model calculates them independently but based on the same intrinsic scattering mechanism parametrized by the parameter λ. The increment of the number of scattering events is mimicked by the increase of the electron temperature. Consequently, the relation between the ultrafast demagnetization and precession remains valid but with a temperature-dependent correction. If this relation is confirmed experimentally, a unique intrinsic coupling parameter means that the same main microscopic mechanism is acting on both time scales. This would also confirm the validity of the LLB model. In the present paper we will show that the analysis of the available experimental data seems to indicate this possibility, at least in pure transition metals such as Ni or Co and in the rare-earth metal Gd. We did not find validity for the corresponding relation in Fe.

Up to now only a classical version ($S \to \infty$) of the LLB equation was used to model ultrafast demagnetization processes.[20–22,25] In the present paper we show the important role of the choice of the quantum spin value, resulting in the differences in the corresponding longitudinal relaxation times. We also investigate the influence of coupling to the bath parameter on the ultrafast magnetization dynamics rates and

show that this parameter, being the only free parameter in the LLB model, defines to a large extent the diversity of different materials. The influence of other parameters is also discussed.

The paper is organized as follows. In Sec. II we present the quantum LLB model and its main features for different spin values S. In Sec. III we present results on the modeling of the demagnetization processes within LLB models with different choices of the quantum spins number S and of the intrinsic scattering mechanisms. In Sec. IV we present our attempts to link the ultrafast magnetization dynamics rates in transition metals and Gd and make a comparison with available experimental data. A good agreement validates the future use of LLB micromagnetics. Section V concludes the paper. In the Appendix we demonstrate the equivalence of the LLB model with $S = 1/2$ and the M3TM model by Koopmans *et al.*[26]

II. THE LANDAU-LIFSHITZ-BLOCH MODEL WITH QUANTUM SPIN NUMBER S

The LLB equation for a quantum spin interacting with an environment was derived from the density matrix equation approach.[29] Spin-spin interactions were taken into account in the mean-field approximation, by considering that the exchange field is the strongest one acting in the system. The resulting dynamical equation interpolates between the standard micromagnetics (the macroscopic Landau-Lifshitz-Gilbert equation) at low temperatures and the Bloch equation (at high temperatures). Unlike the traditional Bloch equation, which is widely used in the description of the nuclear magnetic resonance, the LLB equation describes the dynamics of a strongly coupled system.

The macroscopic ("micromagnetic") equation for the magnetization dynamics, valid at all temperatures, is written in the following form:

$$\dot{\mathbf{n}} = \gamma[\mathbf{n}\times\mathbf{H}_{\text{eff}}] + \frac{\gamma\alpha_{\parallel}}{n^2}[\mathbf{n}\cdot\mathbf{H}_{\text{eff}}]\mathbf{n} - \frac{\gamma\alpha_{\perp}}{n^2}[\mathbf{n}\times(\mathbf{n}\times\mathbf{H}_{\text{eff}})], \tag{1}$$

where γ is the ferromagnetic ratio, T is the bath temperature, $n = M/M_e(T) = m/m_e$ is the reduced magnetization, normalized to the equilibrium value M_e at given temperature T, and $m = M/M_e(T = 0K)$. The internal field $\mathbf{H}_{\text{int}}$ contains all usual micromagnetic contributions (Zeeman, anisotropy, exchange, and magnetostatic) and is augmented by the contribution coming from the temperature,

$$\mathbf{H}_{\text{eff}} = \mathbf{H}_{\text{int}} + \frac{m_e}{2\widetilde{\chi}_{\parallel}}(1-n^2)\mathbf{n}, \tag{2}$$

where $\widetilde{\chi}_{\parallel}(T) = \partial m/\partial H$ is the longitudinal susceptibility. The LLB equation contains temperature-dependent material-specific parameters. These can be taken from the multiscale description, parametrizing the Heisenberg Hamiltonian through *ab initio* models[21] and evaluating the temperature dependence of macroscopic parameters,[37,38] or simply measured experimentally. In the present paper they are calculated within the mean-field approach.[39] In particular, the temperature-dependent magnetization was taken from the Billouin function B_S for the corresponding spin S and the longitudinal susceptibility reads

$$\widetilde{\chi}_{S,\parallel}(T,H) = \frac{\mu_{\text{at}}}{S^2 J_0}\frac{\beta S^2 J_0 B_S'}{1-\beta S^2 J_0 B_S'}. \tag{3}$$

where $\beta = 1/(k_B T)$, k_B is Bolzmann's constant, μ_{at} is the atomistic moment, $J_0 = zJ$, J is the exchange parameter, and z is the number of nearest neighbors.

The LLB equation contains two relaxational parameters: transverse $\alpha_{\perp}$ and longitudinal $\alpha_{\parallel}$, related to the intrinsic coupling-to-the-bath parameter λ. In the quantum description the coupling parameter λ contains the matrix elements representing the scattering events and, thus, is proportional to the spin-flip rate due to the interaction with the environment. This parameter, in turn, could be temperature dependent and, in our opinion, it is this microscopic parameter which should be related to the Gilbert parameter calculated through *ab initio* calculations as in Refs. 40 and 41, since the contribution coming from the spin disordering is not properly taken into account in these models.

In the quantum case the temperature dependence of the LLB damping parameters is given by the following expressions:

$$\alpha_{\parallel} = \frac{\lambda}{m_e}\frac{2T}{3T_C}\frac{2q_S}{\sinh(2q_S)} \underset{S\to\infty}{\Longrightarrow} \frac{\lambda}{m_e}\frac{2T}{3T_C}, \tag{4}$$

$$\alpha_{\perp} = \frac{\lambda}{m_e}\left[\frac{\tanh(q_S)}{q_S} - \frac{T}{3T_C}\right] \underset{S\to\infty}{\Longrightarrow} \frac{\lambda}{m_e}\left[1-\frac{T}{3T_C}\right], \tag{5}$$

with $q_S = 3T_C m_e/[2(S+1)T]$, where S is the quantum spin number and T_C is the Curie temperature. In the case $S\to\infty$ the damping coefficients have the forms used in several previously published works;[39] these are suitable for the comparison with the Langevin dynamics simulations based on the classical Heisenberg Hamiltonian and in agreement with them.[21,28]

Equation (1) is singular for $T \geqslant T_C$; in this case it is more convenient to use the LLB equation in terms of the variable $m = M/M_e(T = 0\text{ K})$.[28] The corresponding LLB equation is indistinguishable from Eq. (1) but with different relaxational parameters $\widetilde{\alpha}_{\parallel} = m_e\alpha_{\parallel}$, $\widetilde{\alpha}_{\perp} = m_e\alpha_{\perp}$, and $\widetilde{\alpha}_{\perp} = \widetilde{\alpha}_{\parallel}$ for $T \geqslant T_C$; in this case the contribution of temperature to $\mathbf{H}_{\text{eff}}$ [the second term in Eq. (2)] is $(-1/\widetilde{\chi}_{\parallel})[1 - 3T_C m^2/5(T - T_C)m]\mathbf{m}$. Although this formulation is more suitable for modeling the laser-induced demagnetization process, during which the electronic temperature is usually raised higher than T_C, it is the expression (5) which should be compared with the transverse relaxation parameter α_{LLG} due to the similarity of the formulation of Eq. (1) with the macromagnetic LLG equation. In the classical case and far from the Curie temperature, $T \ll T_C$, $\lambda \approx \alpha_{\perp} \approx \widetilde{\alpha}_{\perp}$ (α_{LLG}).

The most important feature of the LLB equation is the presence of two relaxational terms: longitudinal and transverse. As a result of the consideration of atomic spin-spin interactions, these macroscopic parameters are temperature dependent. In the LLB model the nature of the longitudinal and the transverse relaxation differs from the point of view of characteristic spin-wave frequencies. The transverse relaxation (known as the LLG damping) is basically the relaxation of the ferromagnetic resonance (FMR) mode. The contribution of other spin-wave modes is reduced to the

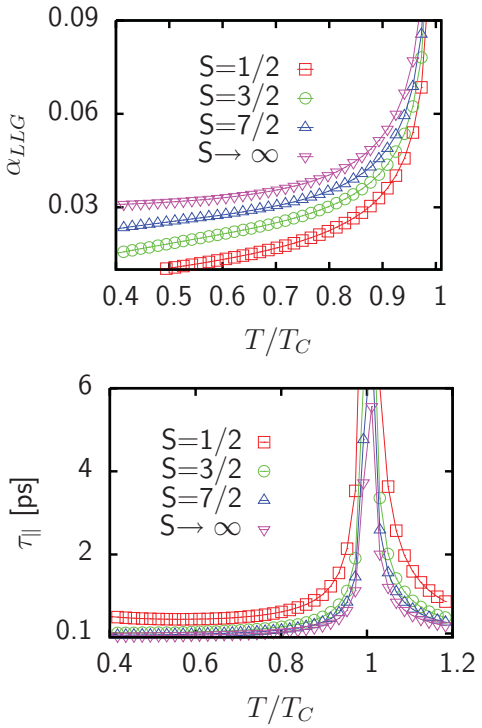

FIG. 2. (Color online) (Top) The transverse damping parameter $\alpha_\perp$ ($\alpha_{\rm LLG}$) as a function of temperature within the LLB model for different spin values S. The intrinsic coupling parameter was set to $\lambda = 0.03$. (Bottom) The longitudinal relaxation time $\tau_\|$ as a function of temperature within the LLB model for different spin values S. The temperature-dependent magnetization and the longitudinal susceptibility $\widetilde{\chi}_\|$ were evaluated in both cases in the MFA approach using the Brillouin function.

thermal averaging of the micromagnetic parameters and the main effect comes from the decrease of the magnetization at high temperature. Consequently, the transverse damping parameter increases with temperature (see Fig. 2), consistent with atomistic modeling results[28] and well-known FMR experiments.[42,43]

In contrast, the main contribution to the longitudinal relaxation comes from the high-frequency spin waves. This process occurs in a strong exchange field. As a result, the longitudinal relaxation time (the inverse longitudinal relaxation rate) is much faster and increases with temperature; this effect is known as critical slowing down (see Fig. 2). This slowing down has been shown to be responsible for the slowing down of the femtosecond demagnetization time τ_M as a function of laser pump fluence.[19,23] The characteristic longitudinal time scale is defined not only by the longitudinal damping parameter (4) but also by the temperature-dependent longitudinal susceptibility $\widetilde{\chi}_\|(T)$,[28] according to the following equation:

$$\tau_\|(T) = \frac{\widetilde{\chi}_\|(T)}{\gamma \widetilde{\alpha}_\|(T)}. \tag{6}$$

Note that $\widetilde{\chi}_\|(T)$ is a function of magnetic moment $\mu_{\rm at}$ and the exchange parameter $J \propto T_C$; it diverges at T_C and at $T > T_C$ $\widetilde{\chi}_\|(T) \propto \mu_{\rm at}/J$.

As can be observed in Fig. 2 the transverse relaxation parameter $\alpha_\perp(\alpha_{\rm LLG})$ and the longitudinal relaxation time $\tau_\|$ have a strong dependence on the quantum spin number S. Particularly, quite different relaxation rates occur for the two extreme cases $S = 1/2$ and $S = \infty$.

III. RESULTS

A. Ultrafast magnetization dynamics within the LLB approach coupled to the two-temperature model

For modeling ultrafast demagnetization we have to specify the origin of the external bath whose role is to produce an energy input. In the spirit of Refs. 20–23 and 26 the modeling of ultrafast magnetization dynamics is based on some reasonable assumptions about the energy transfers taking place among different subsystems; electrons, phonons, and spins. The 2T model assumes that the absorbed energy from the laser pump pulse goes to the electron system, which thermalizes ($\gtrsim$10 fs) to an internal quasiequilibrium distribution at a well-defined temperature T_e, whereas there is still a nonequilibrium energy transfer between electrons and the lattice, which is also assumed to be in a local thermal quasiequilibrium with temperature T_p. Finally, the electron-phonon coupling, $G_{\rm ep}$, drives both systems to a final common temperature. Within this model[16,44–46] the electron and phonon dynamics is described by two differential equations:

$$\begin{aligned} C_e \frac{dT_e}{dt} &= -G_{\rm ep}(T_e - T_p) + P(t), \\ C_p \frac{dT_p}{dt} &= G_{\rm ep}(T_e - T_p), \end{aligned} \tag{7}$$

where $C_e = \gamma_e T_e$ ($\gamma_e = {\rm const}$) and C_p are the specific heats of the electrons and the lattice. The Gaussian source term $P(t)$ is a function which describes the laser power density absorbed in the material. The 2T model is external for the LLB dynamics and can be checked from the measured reflectivity for some materials such as Ni.[23] The dynamics of the electron temperature can also be measured directly in the time-resolved photoemission experiment.[47]

In all previous works on the modeling of ultrafast processes within the LLB model as well as within the atomistic LLG approach,[19–25] it has been assumed that the bath is produced by the electron systems and thus $T = T_e$. This idea follows along the lines of a pure electronic spin-flip mechanism and has been shown to adequately describe ultrafast dynamics in relation to experiments. The possibility of an intrinsic temperature dependence of the spin-flip probability is normally disregarded, under the assumption that $\lambda = {\rm const}$. Therefore, in this approach the longitudinal relaxation time $\tau_\| \sim \widetilde{\chi}_\|/\lambda T_e$ [see Eq. (6)] is defined by the dynamics of the electron temperature T_e, until a temperature close to the Curie temperature where the critical slowing down, provided by the longitudinal susceptibility $\widetilde{\chi}_\|$, starts to play a role.

Recently, Koopmans *et al.* have used a similar approach to describe ultrafast demagnetization dynamics,[26] called the M3TM model, obtained through the general master equation for the dynamics of the populations of a two-level system (in which spin $S = 1/2$ was used) with the spin-flip probability

of the phonon-mediated EY scattering events, a_{sf}. The M3TM model reads

$$\frac{dm}{dt} = Rm\frac{T_p}{T_C}\left[1 - m\coth\left(\frac{mT_C}{T_e}\right)\right]. \quad (8)$$

Here R is a material-specific parameter linearly proportional to the spin-flip probability: $R \sim a_{sf}$. Equation (8) is coupled to the 2T model (7). The use of the M3TM model has allowed the values of R (and, thus a_{sf}) in Ni, Co, and Gd (Ref. 26) to be extracted from the experimental ultrafast demagnetization curves.

In the Appendix, we rewrite the M3TM equation (8) in the form of the LLB ($S = 1/2$) equation and show that in this case

$$\lambda = \frac{3R}{2\gamma}\frac{\mu_{at}}{k_B T_C}\frac{T_p}{T_e} = \lambda_0\frac{T_p}{T_e}, \quad (9)$$

Thus, the Koopmans' model coincides with the LLB equation with $S = 1/2$ where the Elliott-Yafet scattering mechanism is incorporated from the beginning in its functional form. Consequently, if a phonon-mediated EY process was acting, this would correspond to the use of a temperature-dependent coupling rate (9) in the LLB equation, in contrast to previous works with $\lambda = \text{const}$.

Oppositely to the pure electronic process, in the case of a phonon-mediated EY process, the longitudinal relaxation time scale is defined by the dynamics of the phonon temperature, leading to $\tau_\parallel \sim \widetilde{\chi}_\parallel(T_e)/RT_p$, again at electron temperatures not close to T_C where the critical slowing down starts to play an important role. The linear dependence of demagnetization rate in T_p originates from the linear increase of the phonon occupation number n_E with temperature $n_E \sim T_p$ within the Einstein model, since $\hbar\omega_E \ll k_B T_p$ is assumed in the M3TM model. In contrast, at low temperatures, not considered in Eq. (8), we would get $\tau_\parallel \sim 1/T_p^3$.

Therefore, in the phonon-mediated EY picture, in Ref. 26 the classification of materials on the basis of the "magnetic interaction strength" parameter μ_{at}/J was proposed. This is in agreement with the LLB model [Eq. (6)]. Indeed, the longitudinal susceptibility in Eq. (6) is defined by the values of the atomic moment μ_{at} and J and by the fact that this function rapidly increases with temperature and diverges close to $T_C \propto J$. At $T \gtrsim T_C$ one obtains a simple linear relation[28] $\widetilde{\chi}_\parallel \propto \mu_{at}/J$, thus showing the dependence of the demagnetization rate on this parameter, as suggested in Ref. 26. However, we should note also the importance of the microscopic spin-flip rate $\lambda \sim a_{sf}$.

We now present modeling of the ultrafast magnetization dynamics following the laser pulse excitation using the LLB model coupled to the electron temperature T_e. We perform simultaneous integration of Eqs. (1) and (7) with the material-specific parameters taken from Refs. 23 (Ni) and 26 (Gd) and initial condition $M(t = 0) = M_e(300\text{ K})$. The model adequately describes all three stages of the ultrafast magnetization dynamics rates: subpicosecond demagnetization, picosecond recovery, and subnanosecond precession[22,23] (see Fig. 1).

The most important parameter defining the diversity of the ultrafast demagnetization in different materials is the coupling to the bath parameter λ. Thus, it is natural first to investigate qualitatively its influence. In Fig. 3 we show the diversity of magnetization dynamics for various values of the coupling parameter λ, chosen to be independent of temperature. The largest value of λ approximately corresponds to that of the transition metals while the smallest one corresponds to rare earths and half metals. As can be clearly observed, for relatively large values of the spin-flip rate, corresponding to transition metals, the magnetization dynamics can partially follow the electronic temperature, showing a picosecond time scale magnetization recovery. This does not happen for small values of λ and these materials do not recover their magnetization even at the 100-ps time scale. Thus this parameter defines the diversity of the demagnetization rates to a greater extent than the ratio μ_{at}/T_C, suggested in Ref. 26.

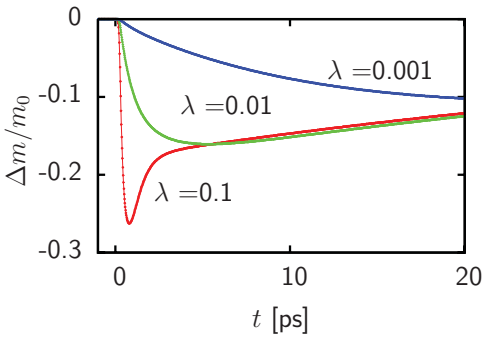

FIG. 3. (Color online) The result of integration of the LLB model ($S \to \infty$) with different parameters λ (increasing from top to the bottom). In this case the the 2T model parameters were taken from Ref. 23 with laser fluence $F = 30\,\text{mJ/cm}^2$. Other material parameters were kept constant and as for Ni.

B. Ultrafast demagnetization rates in different materials

In this section we qualitatively discuss the main parameters governing the ultrafast demagnetization rates in different materials within the LLB model. Note that subpicosecond ultrafast demagnetization generally speaking is not exponential and cannot be described in terms of one relaxation time τ_M. To comply with the existing approaches, we still discuss the demagnetization rate in terms of a unique parameter τ_M.

The magnetization dynamics is determined by a large extent by the dynamics of the bath. However, it is clear that it can only follow the dynamics of the bath temperature if $\tau_{||} \sim 100$ fs is faster than the characteristic time scale of the electron dynamics. At the femtosecond time scale the magnetization dynamics is always delayed with respect to the electrons and phonons. At temperatures close to the Curie temperature, the magnitude $\tau_{||}$ experiences a critical slowing down, and thus the characteristic time scale τ_M is also slowed. Thus the value of $\tau_{||}$ defines the magnetic system response.

It is clear that, independently of the nature of the spin-flip mechanism, the most important parameter determining the value of $\tau_{||}$ remains the material-specific intrinsic scattering rate parameter λ. For the ultrafast dynamics this parameter substitutes the Landau-Lifshitz-Gilbert parameter α_{LLG}, which is normally extracted from the experiment. Similarly, λ at the present state of the art should be extracted from the experimental measurements although, in theory, it can be also calculated from the *ab initio* approach, similar to how it was

TABLE I. The data for ultrafast magnetization dynamics rate parameters for three different metals from ultrafast demagnetization rates and from FMR mesurements. The third column presents the demagnetization parameter R from Ref. 26, corrected in the case of Gd for spin $S = 7/2$. The fourth column presents the value of the λ_0 parameter, as estimated from the M3TM model[26] and Eq. (9). The fifth column presents the data for $\alpha_\perp$ estimated via the LLB model [Eq. (5)] and the λ_0 value from the third column, at room temperature $T = 300$ for Co and Ni and at $T = 120$ K for Gd. The last column presents the experimentally measured Gilbert damping collected from different references.

Material	S	R (Ref. 48)	λ_0	$\alpha_\perp$	α_{LLG}
Ni	1/2	17.2	0.0974	0.032	0.019[48]–0.028[43]
Co	1/2	25.3	0.179	0.025	0.006[49]–0.011[50]
Gd	7/2	0.009	0.0015	0.00036	0.0005[33]

done for the Elliott-Yafet process.[14] The available values of λ are presented in Table I. The value of λ for Gd was found to be 1/60 that of Ni (see Table I). Such a small value of the spin-flip rate in Gd can be qualitatively understood if we recall that magnetism in Gd is defined by the half-filled $4f$ shell electrons while the laser primarily excites $5s6d$ electrons. This slow energy transfer delays the spin-flip processes. Compare the qualitative differences observed in Fig. 3 for transition metals with small λ and Fig. 4 for Gd.

Another parameter strongly influencing the demagnetization rates is the electron-phonon coupling G_{ep} defining the rate of the electron-phonon temperatures equilibration time τ_E. Indeed, in Ref. 26 the value of G_{ep} was reported to be 20 times larger for Ni than for Gd. The small values of the two parameters ensure the correct modeling of the experimentally observed ultraslow demagnetization rates in TbFe alloy,[51] Gd,[52] and half metals[53] and the two demagnetization time scales[26,52] are also well reproduced (see Fig. 4). Within this model the two time-scale processes consist of a relatively fast demagnetization on the order of ~1 ps (however much slower than ~100 fs in Ni), defined by the electron temperature and small value of λ, followed by a much slower process due to a slow energy transfer from the electron to the lattice system.

As mentioned in the previous section, the phonon-mediated EY mechanism predicts the coupling to the bath parameter λ to be dependent on the ratio between the phonon and electron

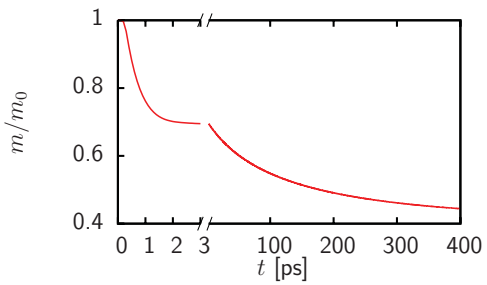

FIG. 4. (Color online) The result of integration of the LLB model ($S \to \infty$) with constant $\lambda = 0.0015$ (see Table I). In this case the 2T model parameters were taken from Ref. 26 corresponding to Gd. The laser fluence was taken to be $F = 30$ mJ/cm^2.

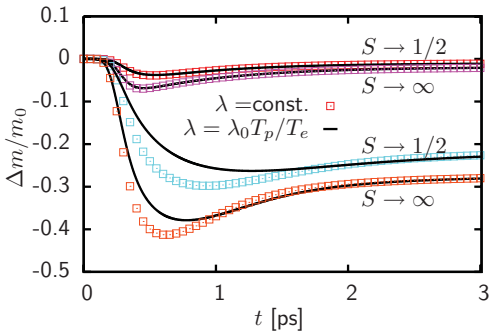

FIG. 5. (Color online) Magnetization dynamics during the laser-induced demagnetization process calculated within the LLB model with different spin numbers and for two laser fluences $F =$ 10 mJ/cm^2 (upper curves) and $F = 40$ mJ/cm^2 (bottom curves). Ni parameters from Ref. 23 were used. The symbols are calculated with the LLB equation with the intrinsic damping parameter using a constant $\lambda_0 = 0.003$ value, and the solid lines with the LLB equation and the intrinsic coupling with the temperature-dependent $\lambda = \lambda_0(T_p/T_e)$.

temperature through the relation (9). In Fig. 5 we present the magnetization dynamics for Ni evaluated for two laser pulse fluences, assuming various values of the spin S and temperature-dependent and independent λ values. Note the quite different demagnetization rates at high fluence for two limiting cases $S = 1/2$ (used in Ref. 26) and $S = \infty$ (used in Ref. 23). The differences in the choice of the mechanism are pronounced at high pump fluence but are not seen at low fluence. One can also hope that in the experiment it would be possible to distinguish the two situations. Considering the experimental data from Ref. 26 for Ni for high fluence, we have found that the case of the temperature-dependent $\lambda = \lambda_0(T_p/T_e)$ can be equally fitted with the temperature-independent $\lambda \approx \lambda_0/2$. Since this is within the discrepancy between the theoretical and experimental values, it does not allow us to answer definitely which mechanism is acting. We conclude that acquiring more experimental data promoting one or another intrinsic mechanism and with varying laser fluence is necessary.

IV. LINKING DIFFERENT TIME SCALES

Since longitudinal relaxation occurs under a strong exchange field and transverse relaxation occurs under an external applied and/or anisotropy field, their characteristic time scales are quite different. However, the LLB equation provides a relation between the ultrafast demagnetization (longitudinal relaxation) and the transverse relaxation (ordinary LLG damping parameter) via the parameters λ for the case $\lambda =$ const or λ_0 for the case $\lambda = \lambda_0(T_p/T_e)$. By separate measurements of the two magnetization dynamics rates, relations (5) and (6) given by the LLB theory could be checked. This can provide validation of the LLB model, as well as the answer to the question of whether the same microscopic mechanism is acting on femtosecond and picosecond time scales. Unfortunately, the damping problem in ferromagnetic materials is very complicated and the literature reveals the diversity of measured values in the same material, depending on the preparation

conditions, substrate, and thin-film thickness. It has been recently demonstrated[54] that the damping of the laser-induced precession coincides with that measured by FMR in transition metals. Thus the two magnetization dynamics rates could be measured independently by means of the ultrafast laser pump-probe technique.[55]

To have a definite answer making measurements on the same sample is highly desired. The measurements of both $\alpha_\perp$ and τ_M are available for Ni (Ref. 23) where an excellent agreement between ultrafast magnetization dynamics rates via a unique temperature-independent parameter $\lambda = 0.04$ has been reported.[23] The results of the systematic measurements of τ_M are also available for Ni, Co, and Gd,[26] as well as for Fe.[56] The next problem which we encounter here is that the demagnetization rates strongly depend on the spin value S, as is indicated in Figs. 2 and 5. The use of the $S = 1/2$ value[26] or $S = \infty$ value[23] is quite arbitrary and these values do not coincide with the atomic spin numbers of Ni, Co, and Gd. Generally speaking, for metals the spin value is not a good quantum number. The measured temperature dependence of magnetization, however, is well fitted by the Brillouin function with $S = 1/2$ for Ni and Co and $S = 7/2$ for Gd.[57] These are the values of S which we use in Table I.

In Table I we present data for the coupling parameter λ_0 extracted from Ref. 53 based on the M3TM model and within the EY mechanism. Differently from that article, for Gd we corrected the value of the parameter R to account for a different spin value by the ratio of the factors, i.e., $R^{S_1} = (f_{S_2}/f_{S_1})R^{S_2}$ with

$$f_S = \frac{2q_S}{\sinh(2q_S)} \frac{1}{m_{e,S}^2 \chi_\parallel^S}, \tag{10}$$

where the parameters are evaluated at 120 K using the MFA expressions for each spin value S. Using the data presented in Table I, we estimated the value of the Gilbert damping parameter $\alpha_\perp$ through formula (5) at 300 K (for Ni and Co) and at 120 K for Gd. Note that for temperature-independent $\lambda = \lambda_0$ the resulting λ_0 and $\alpha_\perp$ values should be divided by a factor of two for Ni and Co. The last column presents experimental values for the same parameter found in the literature for comparison with the ones in the fifth column, estimated through measurements of the ultrafast demagnetization times τ_M and the relation provided by the LLB equation.

The results presented in Table I demonstrate quite a satisfactory agreement between the values extracted from the ultrafast demagnetization time τ_M and the Gilbert damping parameter $\alpha_\perp$ via one unique coupling-to-the-bath parameter λ. The agreement is particularly good for Ni, indicating that the same spin-flip mechanism is acting on both time scales. This is true for both experiments in Refs. 23 and 26. For Co the value is somewhat larger. However, if the temperature-independent $\lambda = \lambda_0/2$ was used, the resulting value would be half as large and the agreement would be again satisfactory. For Ni this would also be within the expected discrepancy among measured FMR values. Note that the results presented in the table are for bulk systems. For thin films an enhancement of the damping by more than by a factor of 2 has been reported.[58,59] We note that no good agreement was obtained for Fe. The reported damping values[43] are factors of 5–10 smaller than estimated from the demagnetization rates measured in Ref. 56.

V. CONCLUSIONS

The Landau-Lifshitz-Bloch equation provides a micromagnetic tool for the phenomenological modeling of ultrafast demagnetization processes. Within this model one can describe the temperature-dependent magnetization dynamics at arbitrary temperature, including close to and above the Curie temperature. The micromagnetic formulation can take into account the quantum spin number. The LLB model includes the dynamics governed by both the atomistic LLG model and the M3TM model by Koopmans *et al*.[26] In the future it represents a real possibility for temperature-dependent multiscale modeling.[21]

Within this model the ultrafast magnetization dynamics rates could be parametrized through a unique temperature-dependent or temperature-independent parameter λ, defined by the intrinsic spin-flip rate. We have shown that for the phonon-mediated EY mechanism the intrinsic parameter λ is dependent on the ratio between phonon and electron temperatures and therefore is temperature dependent on the femtosecond to several-picosecond time scale. The magnetization dynamics is coupled to the electron temperature through this parameter and on the femtosecond time scale is always delayed in time. The observed delay is higher for higher electron temperature. This is in agreement with the experimental observation that different materials demagnetize at different rates[26,53] and that the process is slowed down with the increase of laser fluence. The LLB equation can reproduce slow demagnetizing rates observed in several materials such as Gd, TbFe, and half metals. This is in agreement with both the phonon-mediated EY picture, since in Gd a lower spin-flip probability was predicted, and also with the inelastic electron scattering picture, since the electron diffusive processes are suppressed in insulators and half metals.[53,60] However, we also stress the importance of other parameters determining the ultrafast demagnetization rates, such as electron-phonon coupling.

The macroscopic damping parameters (longitudinal and transverse) have different natures in terms of the involved spin waves and in terms of the time scales. Their temperature dependence is different; however, they are related by the spin-flip rate. We have tried to check this relation in several transition metals such as Ni, Co, and Fe and the rare-earth metal Gd. A good agreement is obtained in Co and Gd and an excellent agreement in Ni. This indicates that on both time scales the same main microscopic mechanism is acting. In Ni the agreement is good within both the assumptions $\lambda = \lambda_0$ and $\lambda = \lambda_0 T_p/T_e$. In Co the agreement seems to be better with the temperature-independent parameter $\lambda = \lambda_0$, which does not indicate the phonon-mediated EY mechanism. However, given a small discrepancy and the complexity of the damping problem, this conclusion cannot be considered definite. We cannot exclude an additional temperature dependence of the intrinsic spin-flip probability (i.e., the parameter λ_0) for either phonon-mediated EY or exchange scattering mechanisms which were not taken into account. The observed agreement of the perpendicular and transverse relaxation rates, generally

speaking, validates the LLB theory but cannot answer the question of which mechanism is acting.

Finally, Fähnle *et al.*[61] have used the Fermi-surface breathing model to link the conductivity contribution to LLG damping and τ_M. Such a contribution dominates at low temperatures and it gives a linear relation $\tau_M \sim \alpha_{\mathrm{LLG}}$, in contrast to our approach and previous approaches, where $\tau_\parallel \sim 1/\alpha_{\mathrm{LLG}}$. At room temperature both contributions seem to be relevant. In their model the electronic properties are taken into account in a more material-specific way, but leaving the spin fluctuations untreated. At the present state of the art our model does not include the conductivity contribution. In that direction we conclude that both models are complementary and could be combined to produce a better understanding of the present problem.

An open question is the problem of doped permalloy where an attempt to systematically change the damping parameter by doping with rare-earth impurities was undertaken[33] in order to clarify the relation between the LLG damping and the ultrafast demagnetization rate.[32,34] The results are not in agreement with the LLB model. However, in this case we think that the hypothesis of the slow relaxing impurities presented in Ref. 34 might be a plausible explanation. Indeed, if the relaxation time of the rare-earth impurities is high, the standard LLB model is not valid since it assumes an uncorrelated thermal bath. The correlation time could be introduced in the classical spin dynamics via the Landau-Lifshitz-Miyasaki-Seki approach.[62] It has been shown that the correlation time of the order of 10 fs slows down the longitudinal relaxation independently of the transverse relaxation. Thus, in this case, modification of the original LLB model to account for the colored noise is necessary.

ACKNOWLEDGMENTS

This work was supported by the Spanish Ministry of Science and Innovation Project No. FIS2010-20979-C02-02.

APPENDIX

To show the equivalence between the LLB model with $S = 1/2$ and the M3TM model,[26] we compare the relaxation rates resulting from both equations. We start with the M3TM equation

$$\frac{dm}{dt} = -R\frac{T_p}{T_C}\left\{1 - m\coth\left[\left(\frac{T_C}{T_e}\right)m\right]\right\}m, \tag{A1}$$

where we identify the Brillouin function for the case $S = 1/2$, $B_{1/2} = \tanh(q)$ with $q = q_{1/2} = (T_C/T_e)\,m$. Now, we use the identity $B_{1/2} = 2/B'_{1/2}\sinh(2q)$ to write

$$\frac{dm}{dt} = -R\frac{T_p}{T_C}\left[\frac{2}{\sinh(2q)}\right]\left(\frac{1-\frac{B_{1/2}}{m}}{B'_{1/2}}\right)m^2. \tag{A2}$$

We multiply and divide by $q\mu_{\mathrm{at}}\beta$ to obtain

$$\frac{dm}{dt} = -R\frac{T_p}{T_C}\frac{\mu_{\mathrm{at}}}{k_B T_C}\left[\frac{2q}{\sinh(2q)}\right]\left(\frac{1-\frac{B_{1/2}}{m}}{\mu_{\mathrm{at}}\beta B'_{1/2}}\right)m. \tag{A3}$$

We expand around equilibrium $m_e = B_{1/2}(q_e)$ the small quantity $1 - B_{1/2}/m$ to get

$$1 - \frac{B_{1/2}(q)}{m} \cong \frac{\delta m}{m_e}\left[1 - \left(\frac{T_C}{T_e}\right)B'_{1/2}(q_e)\right], \tag{A4}$$

where $\delta m = m - m_e$. Next, we expand m around m_e^2, obtaining

$$m = m_e + \frac{1}{2}\frac{(m^2 - m_e^2)}{m_e} \Longrightarrow \frac{\delta m}{m_e} = \frac{(m^2 - m_e^2)}{2m_e^2} \tag{A5}$$

and

$$\frac{1 - B_{1/2}/m}{\beta\mu_{\mathrm{at}}B'_{1/2}} \approx \frac{1}{2\widetilde{\chi}_\parallel}\frac{(m^2 - m_e^2)}{m_e^2}. \tag{A6}$$

Finally, collecting Eqs. (A3) and (A6) together, we obtain

$$\frac{dm}{dt} = \left(\frac{3R}{2}\frac{\mu_{\mathrm{at}}}{k_B T_C}\right)\frac{2T_p}{3T_C}\frac{2q}{\sinh(2q)}\left[\frac{1}{2\widetilde{\chi}_\parallel}\left(1 - \frac{m^2}{m_e^2}\right)m\right]. \tag{A7}$$

Comparing this to the LLB equation with longitudinal relaxation only and without anisotropy and external fields, we can write Eq. (A7) in terms of **n**:

$$\frac{dn}{dt} = \gamma\frac{\lambda}{m_e}\frac{2T_e}{3T_C}\frac{2q}{\sinh(2q)}H_{\mathrm{eff}} = \gamma\alpha_\parallel H_{\mathrm{eff}}, \tag{A8}$$

where $H_{\mathrm{eff}} = \frac{m_e}{2\widetilde{\chi}_\parallel}(1 - n^2)n$ and

$$\alpha_\parallel = \left[\frac{3R}{2\gamma}\frac{\mu_{\mathrm{at}}}{k_B T_C}\frac{T_p}{T_e}\right]\frac{2T_e}{3T_C}\frac{2q}{\sinh(2q)}. \tag{A9}$$

Thus the Koopmans' M3TM equation is equivalent to the LLB equation with $S = 1/2$ and where the precessional aspects are not considered. The link between them is the identification

$$\lambda = \frac{3R}{2\gamma}\frac{\mu_{\mathrm{at}}}{k_B T_C}\frac{T_p}{T_e}. \tag{A10}$$

As an example we compare the result of the longitudinal relaxation in a numerical experiment for both M3TM and LLB ($S = 1/2$) equations. The system is put in an initial state with $m_z = 1$ and we let it relax toward the equilibrium state at final temperature. The comparison of the results for the temperature $T/T_C = 0.8$ is presented in Fig. 6.

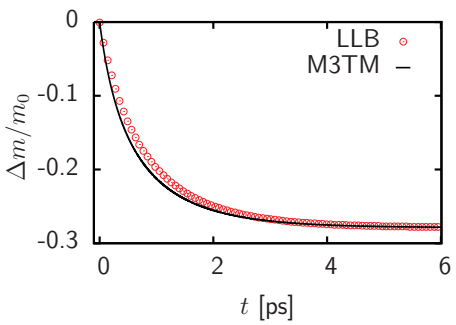

FIG. 6. (Color online) Longitudinal relaxation calculated with M3TM and LLB ($S = 1/2$) models for nickel parameters[23] and $T/T_C = 0.8$.

[1] C. H. Back and D. Pescia, Nature (London) **428**, 808 (2004).

[2] I. Tudosa, C. Stamm, A. B. Kashuba, F. King, H. C. Siegmann, J. Sthör, G. Ju, B. Lu, and D. Weller, Nature (London) **428**, 831 (2004).

[3] E. Beaurepaire, J. C. Merle, A. Daunois, and J.-Y. Bigot, Phys. Rev. Lett. **76**, 4250 (1996).

[4] J. Hohlfeld, E. Matthias, R. Knorren, and K. H. Bennemann, Phys. Rev. Lett. **78**, 4861 (1997).

[5] A. Scholl, L. Baumgarten, R. Jacquemin, and W. Eberhardt, Phys. Rev. Lett. **79**, 5146 (1997).

[6] B. Koopmans, J. M. Ruigrok, F. Dalla Longa, and W. J. M. de Jonge, Phys. Rev. Lett. **95**, 267207 (2005).

[7] A. Kirilyuk, A. Kimel, and Th. Rasing, Rev. Mod. Phys. **82**, 2731 (2010).

[8] C. Stamm, T. Kachel, N. Pontius, R. Mitzner, T. Quast, K. Holldack, S. Khan, C. Lupulescu, E. F. Aziz, M. Wiestruk, H. A. Dürr, and W. Eberhardt, Nat. Mater. **6**, 740 (2007).

[9] J.-Y. Bigot, M. Vomir, and E. Beaurepaire, Nat. Phys. **5**, 515 (2009).

[10] C. Boeglin, E. Beaurepaire, V. Halté, V. López-Flores, C. Stamm, N. Pontius, H. A. Dürr, and J.-Y. Bigot, Nature (London) **465**, 458 (2010).

[11] G. Zhang, W. Hübner, E. Beaurepaire, and J.-Y. Bigot, in *Spin Dynamics in Confined Magnetic Structures I*, Topics in Applied Physics Vol. 83 (Springer-Verlag Berlin, 2002), p. 252.

[12] G. P. Zhang, Y. Bai, W. Hübner, G. Lefkidis, and T. George, J. Appl. Phys. **103**, 07B113 (2008).

[13] G. P. Zhang and W. Hübner, Phys. Rev. Lett. **85**, 3025 (2000).

[14] D. Steiauf and M. Fähnle, Phys. Rev. B **79**, 140401(R) (2009).

[15] M. Krauß, T. Roth, S. Alebrand, D. Steil, M. Cinchetti, M. Aeschlimann, and H. C. Schneider, Phys. Rev. B **80**, 180407(R) (2009).

[16] M. I. Kaganov, I. M. Lifshitz, and L. V. Tanatarov, Sov. Phys. JETP **4**, 173 (1957).

[17] M. B. Agranat, S. I. Ashitkov, A. B. Granovski, and G. I. Rukman, Zh. Eksp. Teor. Fiz. **86**, 1376 (1984).

[18] J. Hohlfeld, S.-S. Wellershoff, J. Güdde, U. Conrad, V. Jähnke, and E. Matthias, Chem. Phys. **251**, 237 (2000).

[19] N. Kazantseva, U. Nowak, R. W. Chantrell, J. Hohlfeld, and A. Rebei, Europhys. Lett. **81**, 27004 (2008),

[20] N. Kazantseva, D. Hinzke, U. Nowak, R. W. Chantrell, and O. Chubykalo-Fesenko, Phys. Status Solidi **244**, 4389 (2007).

[21] N. Kazantseva, D. Hinzke, U. Nowak, R. W. Chantrell, U. Atxitia, and O. Chubykalo-Fesenko, Phys. Rev. B **77**, 184428 (2008).

[22] U. Atxitia, O. Chubykalo-Fesenko, N. Kazantseva, D. Hinzke, U. Nowak, and R. W. Chantrell, Appl. Phys. Lett. **91**, 232507 (2007).

[23] U. Atxitia, O. Chubykalo-Fesenko, J. Walowski, A. Mann, and M. Münzenberg, Phys. Rev. B **81**, 174401 (2010).

[24] N. Kazantseva, D. Hinzke, R. W. Chantrell, and U. Nowak, Europhys. Lett. **86**, 27006 (2009).

[25] K. Vahaplar, A. M. Kalashnikova, A. V. Kimel, D. Hinzke, U. Nowak, R. Chantrell, A. Tsukamoto, A. Itoh, A. Kirilyuk, and T. Rasing, Phys. Rev. Lett. **103**, 117201 (2009).

[26] B. Koopmans, G. Malinowski, F. Dalla Longa, D. Steiauf, M. Fähnle, T. Roth, M. Cinchetti, and M. Aeschlimann, Nat. Mater. **9**, 259 (2010).

[27] D. A. Garanin, Phys. Rev. B **55**, 3050 (1997).

[28] O. Chubykalo-Fesenko, U. Nowak, R. W. Chantrell, and D. Garanin, Phys. Rev. B **74**, 094436 (2006).

[29] D. A. Garanin, Physica A **172**, 470 (1991).

[30] J. S. Hong and D. L. Mills, Phys. Rev. B **62**, 5589 (2000).

[31] T. Balashov, A. F. Takacs, M. Dane, A. Ernst, P. Bruno, and W. Wulfhekel, Phys. Rev. B **78**, 174404 (2008).

[32] J. Walowski, G. Müller, M. Djordjevic, M. Münzenberg, M. Kläui, C. A. F. Vaz, and J. A. C. Bland, Phys. Rev. Lett. **101**, 237401 (2008).

[33] G. Woltersdorf, M. Kiessling, G. Meyer, J.-U. Thiele, and C. H. Back, Phys. Rev. Lett. **102**, 257602 (2009).

[34] I. Radu, G. Woltersdorf, M. Kiessling, A. Melnikov, U. Bovensiepen, J.-U. Thiele, and C. H. Back, Phys. Rev. Lett. **102**, 117201 (2009).

[35] E. Beaurepaire, G. M. Turner, S. M. Harrel, M. C. Beard, J.-Y. Bigot, and C. A. Schmuttenmaer, Appl. Phys. Lett. **84**, 3465 (2004).

[36] M. Djordjevic and M. Münzenberg, Phys. Rev. B **75**, 012404 (2007).

[37] P. Asselin, R. F. L. Evans, J. Barker, R. W. Chantrell, R. Yanes, O. Chubykalo-Fesenko, D. Hinzke, and U. Nowak, Phys. Rev. B **82**, 054415 (2010).

[38] U. Atxitia, D. Hinzke, O. Chubykalo-Fesenko, U. Nowak, H. Kachkachi, O. N. Mryasov, R. F. Evans, and R. W. Chantrell, Phys. Rev. B **82**, 134440 (2010).

[39] D. A. Garanin and O. Chubykalo-Fesenko, Phys. Rev. B **70**, 212409 (2004).

[40] K. Gilmore, Y. U. Idzerda, and M. D. Stiles, Phys. Rev. Lett. **99**, 027204 (2007).

[41] J. Kuneš and V. Kamberský, Phys. Rev. B **65**, 212411 (2002).

[42] Y. Li, K. Baberschke, and M. Farle, J. Appl. Phys. **69**, 4992 (1991).

[43] S. M. Bhagat and P. Lubitz, Phys. Rev. B **10**, 179 (1974).

[44] R. W. Schoenlein, W. Z. Lin, J. G. Fujimoto, and G. L. Eesley, Phys. Rev. Lett. **58**, 1680 (1987).

[45] P. B. Allen, Phys. Rev. Lett. **59**, 1460 (1987).

[46] X. Wang, S. Nie, J. Li, R. Clinite, J. E. Clarck, and J. Cao, Phys. Rev. B **81**, 220301 (2010).

[47] U. Bovensiepen, J. Phys. Condens. Matter **19**, 083201 (2007).

[48] G. Dewar, B. Heinrich, and J. F. Cochran, Can. J. Phys. **55**, 821 (1977).

[49] J. Lindner, I. Barsukov, C. Raeder, C. Hassel, O. Posth, R. Meckenstock, P. Landeros, and D. L. Mills, Phys. Rev. B **80**, 224421 (2009).

[50] B. Heinrich, J. F. Cochran, M. Kowalewski, J. Kirschner, Z. Celinski, A. S. Arrott, and K. Myrtle, Phys. Rev. B **44**, 9348 (1991).

[51] J. W. Kim, K. D. Lee, J. W. Jeong, and S. C. Shin, Appl. Phys. Lett. **94**, 192506 (2009).

[52] M. Wietstruk, A. Melnikov, C. Stamm, T. Kachel, N. Pontius, M. Sultan, C. Gahl, M. Welnet, H. A. Dürr, and U. Bovensiepen, Phys. Rev. Lett. **106**, 127401 (2011).

[53] G. M. Müller *et al.*, Nat. Mater. **8**, 56 (2009).

[54] S. Mizukami, H. Abe, D. Watanabe, M. Oogane, Y. Ando, and T. Miyazaki, Appl. Phys. Exp. **1**, 121301 (2008).

[55] J. Walowski, M. Djordjevic, M. D. Kauffman, B. Lenk, C. Hamann, J. McCord, and M. Münzenberg, J. Phys. D **41**, 164016 (2008).

[56] E. Carpene, E. Mancini, C. Dallera, M. Brenna, E. Puppin, and S. De Silvestri, Phys. Rev. B **78**, 174422 (2008).

[57]B. D. Cullity, *Introduction to Magnetic Materials* (Addison-Wesley, Reading, MA, 1972).
[58]D. Spoddig, R. Meckenstock, J. P. Bucher, and J. Pelzl, J. Magn. Magn. Mater. **286**, 286 (2005).
[59]W. Platow, A. N. Anisimov, G. L. Dunifer, M. Farle, and K. aberschke, Phys. Rev. B **58**, 5611 (1998).
[60]M. Battiato, K. Carva, and P. M. Oppeneer, Phys. Rev. Lett. **105**, 027203 (2010).
[61]M. Fähnle, J. Seib, and C. Illg, Phys. Rev. B **82**, 144405 (2010).
[62]U. Atxitia, O. Chubykalo-Fesenko, R. W. Chantrell, U. Nowak, and A. Rebei, Phys. Rev. Lett. **102**, 057203 (2009).